Identification Of FDA Approved Drugs With Activity Against Lassa Virus- A Computational Drug Repositioning Approach.

Yunusa A[1*] & Bello SO[1]

[1]Department of Pharmacology and therapeutics, Usmanu Danfodiyo University, Sokoto, Nigeria.
Corresponding author email: abdulmajeedyunusa@gmail.com

Abstract

This study was aimed at identifying generic drugs with activity against Lassa virus. It has two components; computational and *in-vitro* studies. The computational study entails sequential screening of all FDA approved drugs (1491) against three protein targets; through structural- and ligand- based pharmacophores screening followed by molecular docking of the selected drugs against the viral targets. Two (2) drugs with the best binding affinities against the viral targets were chosen for an *in-vitro* confirmation of activity. The non-toxic concentrations used for the study were established from MTT cytotoxicity study using C_{max} of the drugs as a guide. Iodixanol and sirolismus had the best binding affinities against the three viral targets. Again, iodixanol and sirolismus produced a concentration dependent viral killing in the antiviral studies. Sirolismus and iodixanol produced significant anti-Lassa virucidal effects (49.7% and 41.6% respectively) at 0.4µg/ml and 4000 µg/ml respectively not different from the effect produced by ribavirin (%VI = 54.0).

Key words: Molecular docking, Pharmacophore-modelling, structure based pharmacophore, ligand based pharmacophore, drug-repositioning, antiviral, viral load.

1.0   Introduction

Infectious diseases are becoming more alarming with high morbidity and mortality in developing countries like Africa (Yamani et al., 2017). Viral infections like Lassa virus are often regarded as incurable and fatal diseases (Yamani et al., 2017). Again, the emergence of drug resistant strains have compromised the efficacy of most antiviral agents; some have troublesome and unbearable side effects while some are less efficacious (Kühnert et al., 2018; Wang et al., 2018). Drug repositioning approach might be a better alternative for discovering more effective and less harmful antiviral agents. The high cost of developing drugs has limited the number of antiviral agents into a short list (Bhandari, 2017). Lassa fever is a deadly hemorrhagic disease of great public health importance (Akpede et al., 2018). The Lassa fever outbreak in Nigeria in 2018 was alarming, as 428 cases with 107 mortalities were recorded within the period of 5 months from January to May, 2018 (Tambo et al., 2018). This was the largest outbreak of Lassa fever (case fatality of 25%) ever reported in Nigeria. Ribavirin, a must win, is the only available drug for Lassa fever.

1.1   Aim of the Study

To identify generic drugs with activity against Lassa virus through *in-silico* screening and wet laboratory confirmation.

1.2   Objectives of the Study
1.   To develop a local database for FDA-Approved drugs and three (3) Lassa viral protein targets.
2.   To screen commercially approved drugs using structural- and ligand-based pharmacophores as templates.
3.   To run a docking simulation of the selected drugs against the three viral targets and select best two (2).
4.   To run an *in-vitro*-antiviral studies of the two (2) selected drugs against Lassa infected Caco-2 cell line.

2.0   Materials and Methods

2.1   Criteria for Viral Targets Selection

The Lassa viral targets were selected based on validated selection criteria and scoring (Ansari et al., 2018). The criteria include: involvement in a critical pathway necessary for the survival and replication of the viruses, confirmed or putative targets of known Antiviral agents, absence of significant cross talk from NCBI blast search, drugability of the target (easily accessible binding site) and site or location of the protein target within virus; either on the cell surface/cytoplasm or inside the nucleus (Sliwoski et al., 2014; Ansari et al., 2018). Targets with score of at least 80 out of 115 were selected and considered as critical in the survival and multiplication of the viruses (Sliwoski et al., 2014).

2.2   Development of Local Database of Viral Protein Targets from Protein DataBank

Protein Data Bank (PDB) is an archive of 3D structures of about 35,000-50,000 biological molecules. Three (3) Lassa viral targets (in PDB text format) necessary for their survival and multiplication were selected and downloaded from the PDB website (www.rcsb.org) and saved in PDB text format. A local Database was created for the viral targets in my personal computer (Smart et al., 2018).

2.3   Development of Local Database for FDA-Approved Drug from DrugBank

A DrugBank is a drug Database that contains more than 4,000 compounds linked to about 14,000 molecular targets. All (1491) FDA-Approved drugs were downloaded from DrugBank website (www.drugbank.ca) and saved in structural data format (SDF) (Wishart et al., 2017).

2.4   Structure-based Pharmacophore Screening

Ligand Scout advanced molecular design software was used to generate structure-based pharmacophore for each viral targets using the target- co-crystalized ligand complex as a template (Ansari et al., 2018).

2.5   Ligand-Based Pharmacophore Screening

Ligand-based pharmacophore was generated using all the co-crystalized ligands for the three different viral targets as templates. The generated ligand-based pharmacophore can be merged or shared similarity pharmacophore (Ansari et al., 2018).

2.6   Screening of FDA-Approved Drugs using the Structural and Ligand-Based Pharmacophores as Templates

The structure and ligand-based pharmacophores were copied to the screening perspective using the copy board widget. Approved drugs downloaded from the DrugBank were loaded to the screening Database using the "create and load screening database". The generated pharmacophores were screened against the approved drugs and the drugs with similar pharmacophores were displayed in the tabular form compatible with excel (Ansari et al., 2018).

2.7   Docking Simulation of the Selected Drugs from Pharmacophore Screening against three (3) Lassa Viral Targets using PyRx Virtual Screening Tool

2.7.1   Importation of macromolecules from the local Database

To import macromolecule from local Database, File > Import molecule was selected, this displays "import molecule wizard" carrying different options. Workspace Tarball > local File was then selected and "Next" button clicked followed by Finish button. Shortly an "Import Completed Successfully" dialog appears, then OK button was clicked. The 3D structure of the macromolecule was displayed in the workspace and the protein ID appears in the "molecule tab" of the navigator panel. Atoms of the macromolecule were viewed in the workspace by deselecting and selecting them in the "molecule tab" of the navigator panel. The macromolecule was inspected in the workspace by right clicking and holding the mouse. The binding site of the co-crystallized area examined, in shape, size, polarity and accessibility (Ellingson and Baudry, 2014).

2.7.2   Importation of ligands from the local database

To import ligands from the local Database, select open babel button in the control panel of the PyRx tool. Clicking the insert new item tab on the upper left hand corner of the open babel panel, a "choose open babel supported file" box appears that takes you to the ligand Database in my personal computer. The ligand of interest was then selected and imported into the PyRx. The selected ligands appear in the open babel results table displaying the drugs ID, formula, weight and LogP. Minimized atomic coordinates of the ligand was created using "the minimize all" widget. The minimized coordinate of the ligands right clicked and different options displayed. The option "Covert all to autodock ligand PDBQT" was selected. The PDPQT format of the ligand appears in the ligand compartment of the autodock navigator area (Ellingson and Baudry, 2014).

2.7.3   Running the molecular docking simulation

The ligands of interest were selected from the autodock widget and "select ligand" button pressed, followed by the forward button. This automatically input the ligands into the ligand list in the control panel of PyRx software. Again, the macromolecules were selected from the autodock widget and "select macromolecule" button pressed followed by the forward button and this automatically input macromolecules into the macromolecule list in the control panel (Ellingson and Baudry, 2014).

To run vina, the "run vina" was clicked, then forward button pressed. Finally "analyze result" was selected then forward button. This displays the binding affinities of the various poses against the ligands. The lower the binding affinities the better the protein-ligand interaction, since molecules interact to conserve energy (Dallakyan and Olson, 2015).

The Analyze results page is where the final docking results were presented. The table was sorted according to the values of the binding energies. The table row was selected one by one to see the corresponding docking pose for each ligand-protein complex in the 3D scene. The numerical results were exported as a Comma-Separated Values (CSV) file compatible with excel (Dallakyan and Olson, 2015).

2.7.4   Selection of the Best two (2) Performing Drugs for In-vitro Antiviral Studies

Two (2) drugs with overall best binding affinities against the nine viral targets were selected for confirmation of activity in the wet laboratory using *in-vitro* cell line based assay. The analytical grade of the selected drugs were purchased from sigma Aldrich.

2.8   In-vitro Model for Lassa Virus

Ten thousand cells/well were cultured in a 24-well plates for 24 hours to achieve 80-90% confluency. Media changed and the cells washed with phosphate buffer solution before addition of viral particles.

> For Caco-2 cells, 1ml of infected supernatant containing 0.092 LogIU/ml of Lassa virus was added to each well.

The infected cells were maintained and propagated in DMEM (Dulbecco's Modified Eagle Medium) medium supplemented with 10% fetal bovine serum (FBS) and 1% penicillin/ streptomycin and incubated at 37°C in a humidified and 5% CO_2 chamber (Farag and Mansour, 2016).

2.9   Intensive In-vitro Antiviral activity of the Two Selected Drugs

Twenty four hour post infection, the cell lines were treated with three graded concentrations of the two selected drugs (in duplicates), DMSO treated and positive controls (in duplicates). The viral RNA were released following lyses of the infected cell lines at 48 hours post treatment. The viral loads for each of the treatment groups were quantified using real time PCR.

2.10   Determination of percentage viral inhibition (%VI)

The percentage viral inhibition for each of tested group was calculated using the formula (Kati et al., 2015):

$$\% \, VI = \frac{VC - VTG}{VC} \times 100$$

Where VC is the viral load of the DMSO treated group

VTG is the viral load of the treated group.

2.11   Determination of IC_{50}

Nonlinear regression analysis curve generated by graph pad prism was used to extrapolate the IC_{50} of each drug against each virus. The IC_{50} is the concentration that produces 50% viral inhibition (Lo et al., 2016).

2.12   Determination of CC_{50}

Nonlinear regression analysis curve generated by graph pad prism was used to extrapolate the CC_{50} of each drug against each cell line. The CC_{50} is the concentration that produces 50% cell line viability (Lo et al., 2016).

2.13   Determination of Selectivity Index (SI)

The selectivity index for each drug against a particular cell line was calculated using the formular (Lo et al., 2016).

$$SI = CC_{50}/IC_{50}$$

2.14   Data Analysis

Data were presented in tables and graphs and were expressed as mean ±SEM. The half- maximal inhibitory concentration (IC_{50}) and half-maximal toxic concentrations (CC50) were extrapolated from a sigmoidal dose-response curve. Statistical differences between the viral loads for the different drug groups and distinct post treatment time points were analyze using a two-way ANOVA followed by Dunnet's multiple comparison tests. The p values of < 0.05 were considered to be statistically significant. All analyses were performed using Graph Pad Prism version 7.

3.0   Results

3.1   Three (3) Selected Protein Targets and their Scores

Three viral protein targets were identified and validated. The total score for each viral target was greater than 80, hence validated (Table 1).

Table 1: Three (3) Selected Protein Targets and their Scores

S/N	Viral protein targets	Critical in the pathway (50)	Putative Antiviral drug target (30)	No signi-ficant crosstalk (15)	Drug ability of the target (10)	Location of target in virus (10)	Total Score (115)
7	Lassa nucleo-protein (3mx5)	50	0	15	10	Surface(10)	85
8	Lassa glycol-protein (4zjf)	50	0	15	10	Surface(10)	85
9	Lassa polymerase (5j1n)	50	30	15	10	Nucleus (5)	110

3.2   Selected Drugs from Structure-based Pharmacophore

Three hundred and eight (209) FDA drugs and fourty three (20) drugs were selected from the structure- and ligand-based pharmacophore screening.

3.3   Best Two (2) Drugs and there Binding Affinities

Iodixanol and sirolismus had the best binding affinities against the three Lassa targets. The binding affinities for each drug against the viral targets were greater than that for the respective co-crystalized ligands (Table 3).

Table 2: List of Best Two (2) Drugs and there Binding Affinities

Ligand	Lassa nucleo protein	Lassa glycol protein	Lassa polymerase
Co-crystalized ligand	-14.5	-10.5	-9.9
Iodixanol	-21.9	-15.2	-16.5
Sirolismus	-20.4	-18.3	-18.6

Pharmacaphores for the Three (3) Viral Targets and the Two Selected Drugs

Hydrogen bond donor (HBD), Hydrogen bond acceptor (HBA), Negative ionisable areas (NI) and hydrophobic interactions (H) were the common structure and ligand-based pharmacophore features, as shown in Figures 1 to 6.
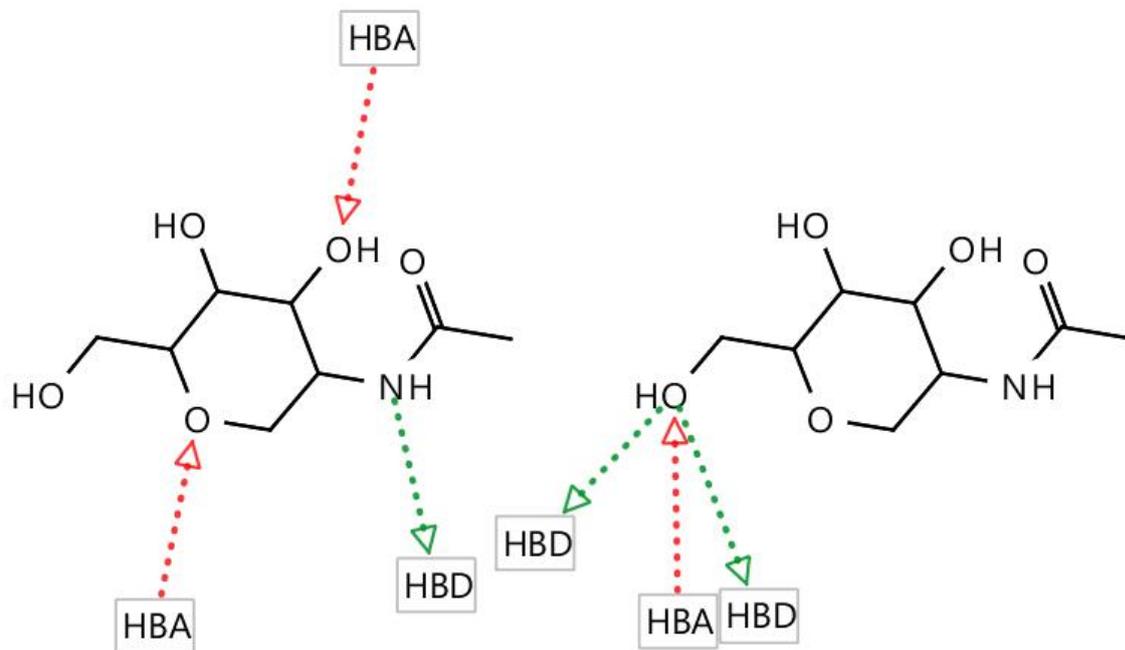
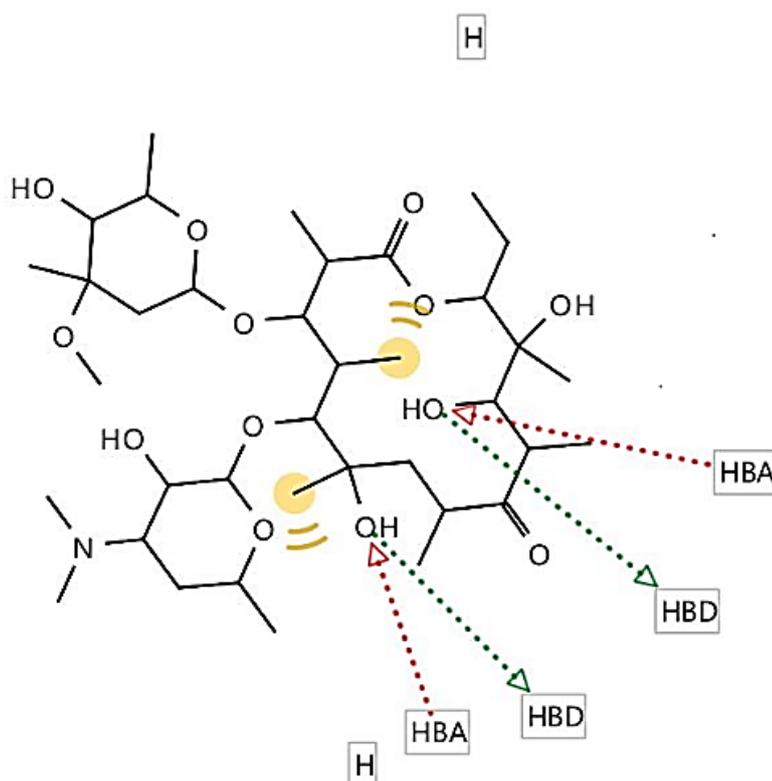*Figure 1:   Structure-based Pharmacophore for Lassa Glycoprotein (4ZJF) –Co-crystalized Ligand Complex*

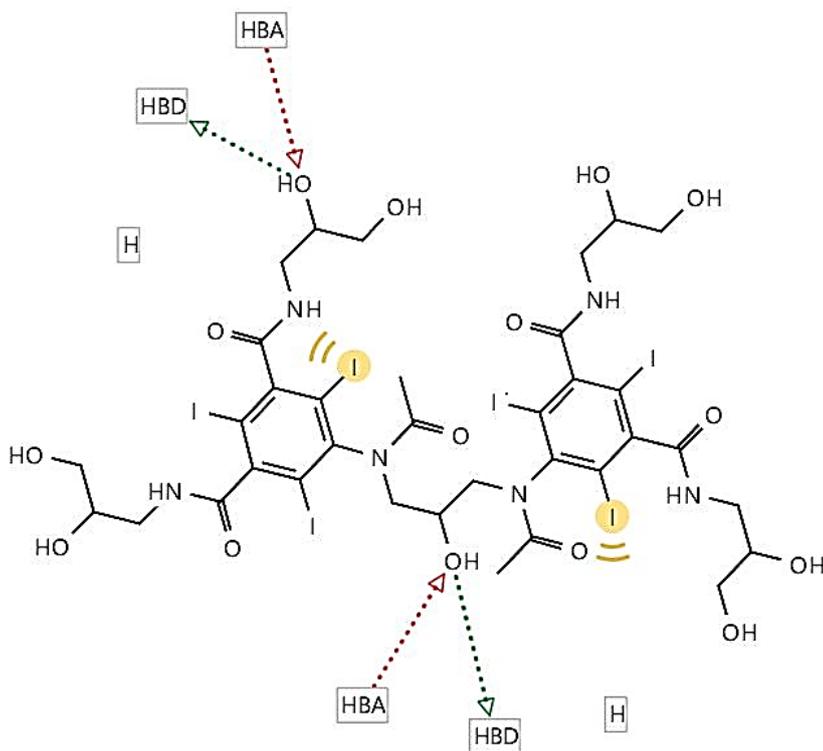*Figure 2:   Generated Pharmacophore for Sirolismus*

Figure 3:   *Generated Pharmacophore for Iodixanol*
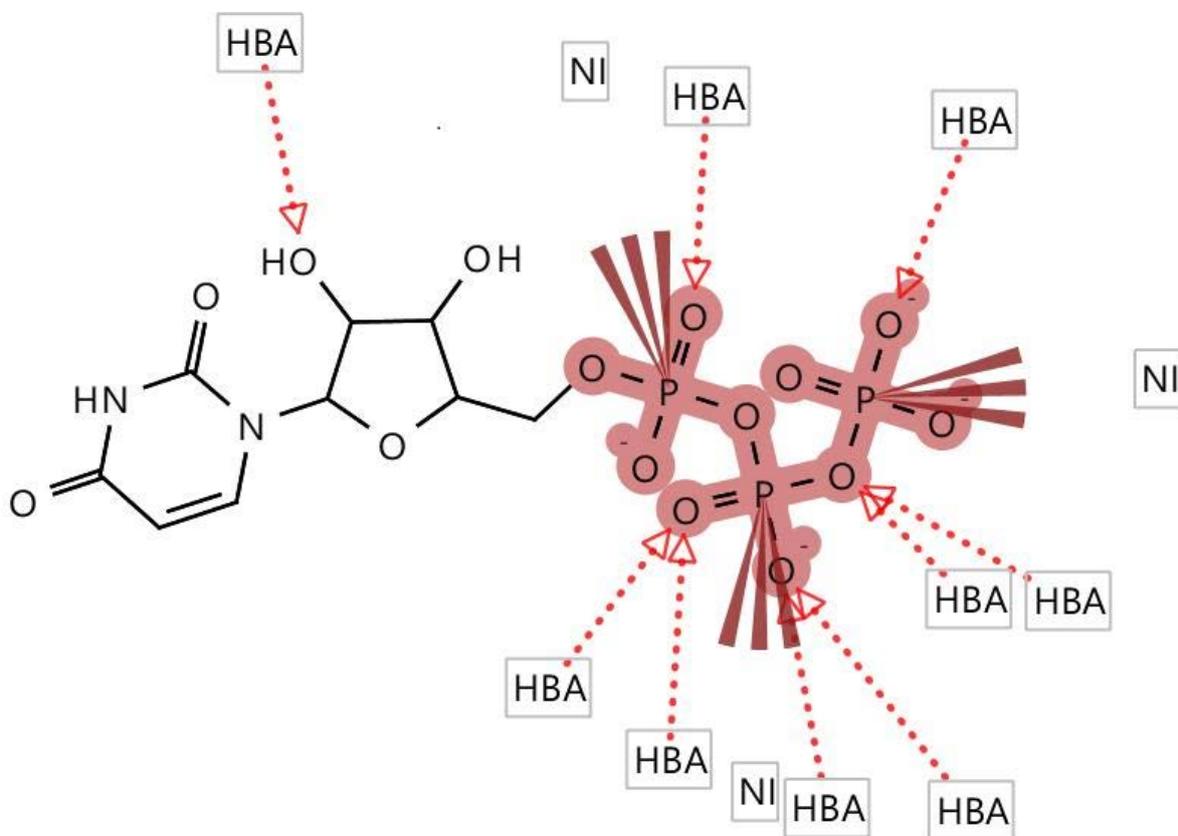

Figure 4:   *Structure-based Pharmacophore for Lassa Nucleoprotein (3MX5) –Co-crystalized Ligand Complex*
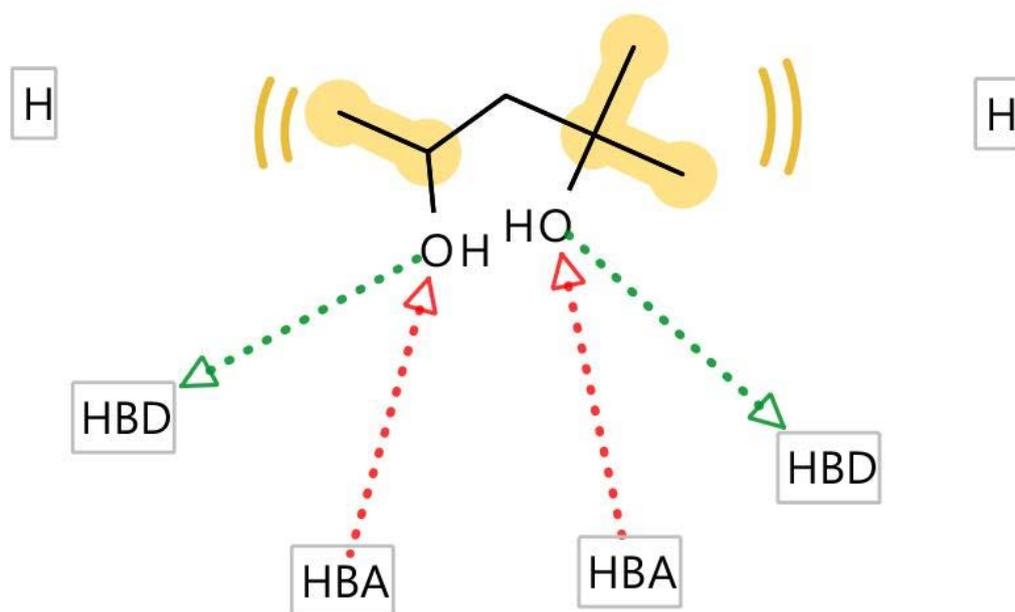
Figure 5:   *Structure-based Pharmacophore for Lassa Polymerase (5J1N) –Co-crystalized ligand complex*
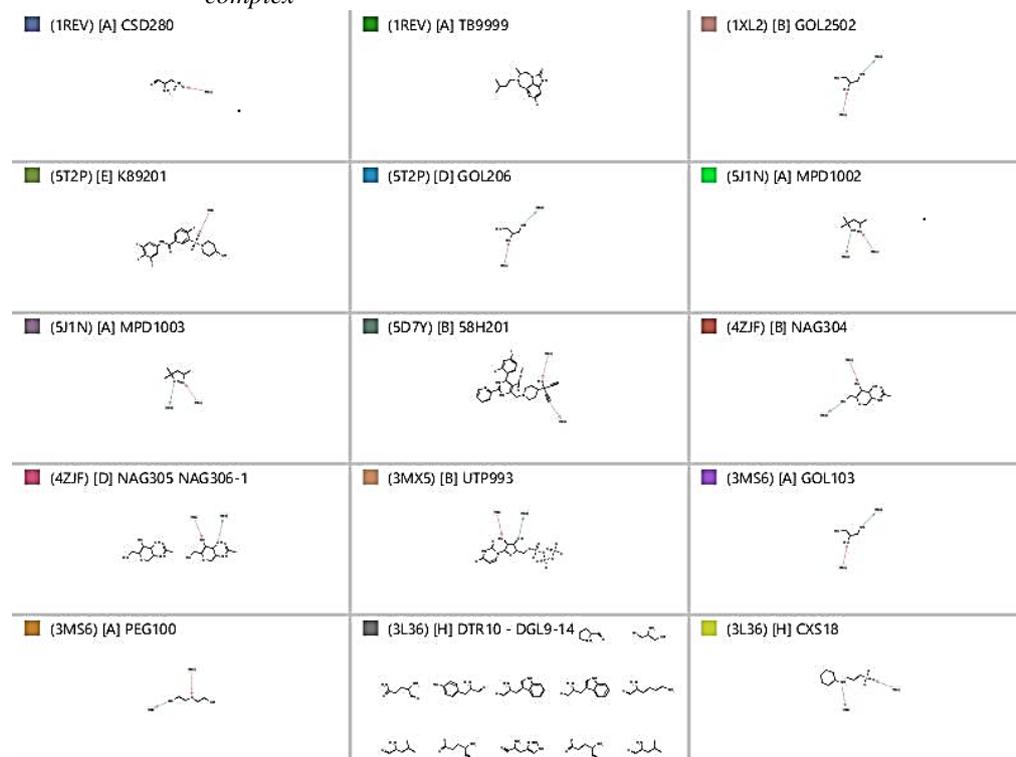

Figure 6:   *Ligand-based Pharmacophore for the Nine (9) Viral Targets*
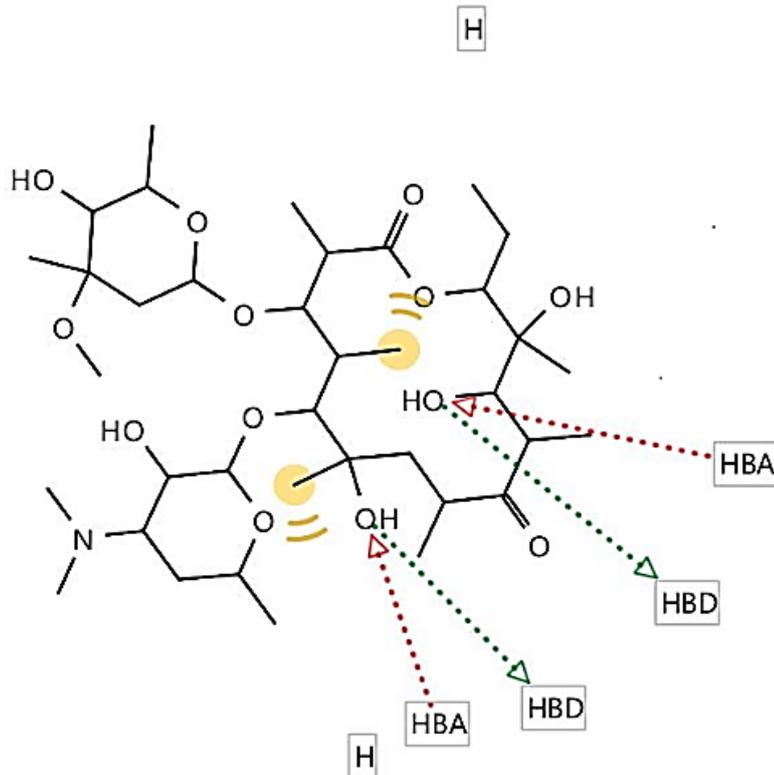
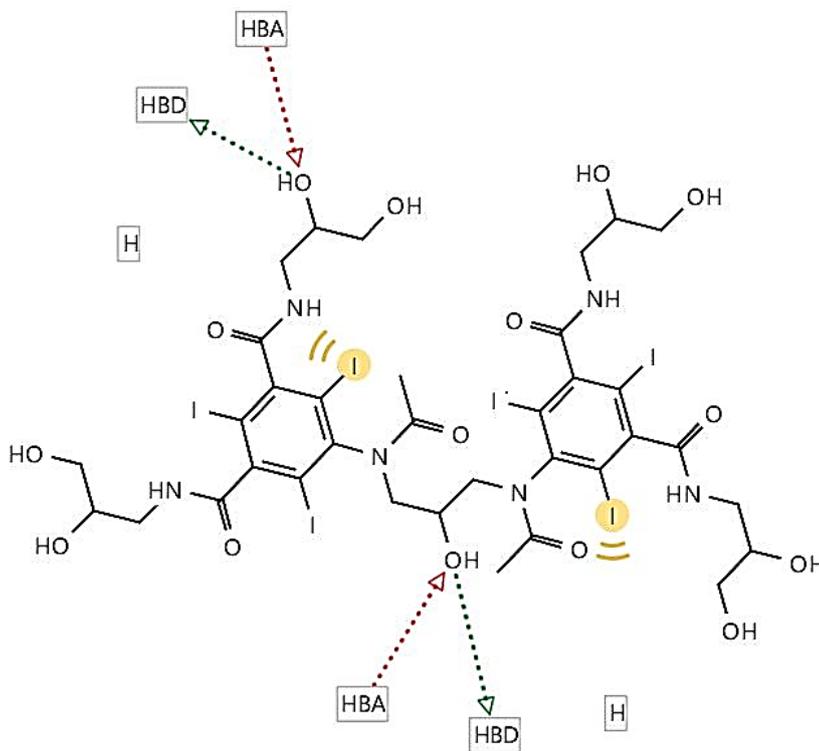*Figure 7:   Generated Pharmacophore for Sirolismus*

Figure 8:   Generated Pharmacophore for Iodixanol

3.5   Three Graded Nontoxic Concentrations of the Two Selected Drugs for the In vitro Antiviral Studies
The three graded non- toxic concentrations for iodixanol and sirolismus from MTT cytotoxicity study were used for the antiviral study. The concentrations of the stock solution for each drug and the volume of stock to make the highest concentrations were calculated. This is to allow easy serial dilution during drug treatment (Table 3).

Table 3:   Three Graded Nontoxic Concentrations of the Two Selected Drugs for the In vitro Antiviral Studies

Drugs	Lowest conc. (μg/ml)	Mid conc. (μg/ml)	Highest conc. (μg/ml)	Conc. Of stock (μg/ml)
Iodixanol	1000	2000	4000	16,000
Sirolismus	0.1	0.2	0.4	100

3.6   In-vitro Virucidal Effects of the Two (2) Selected Drugs against Lassa virus at three Graded Concentrations and at three Post-treatment Time Points

There's a significant difference in the virucidal effect of iodixanol and sirolismus against Lassa when compared to the negative control in all the post-treatment groups except for the effects in the 72 hours post treatment at lowest non-toxic concentrations. The virucidal effect of sirolismus was not significantly different from ribavirin in the 24 hours post treatment groups at mid non-toxic concentrations. Again sirolismus and iodixanol had statistically the same virucidal effect with ribavirin in the 24 and 48 hours post treatment groups at highest non-toxic concentrations. Sirolismus produced a high viral killing effect than iodixanol across the post treatment groups for the three graded concentrations (Table 4).

Table 4:   In vitro Virucidal effects of Iodixanol, Sirolismus and Ribavirin against Lassa virus at three Graded Concentrations at three Post-treatment time points

	Drugs	**24 hours**	**%VI**	**48 hours**	**%VI**	**72 hours**	**%VI**
Lowest Concentration	Iodixanol	0.086 ± 0.001***	5.8	0.086 ± 0.001***	5.8	0.093 ± 0.000***	-1.9
	Sirolismus	0.081 ± 0.000***	11.3	0.081 ± 0.002***	11.4	0.09 ± 0.001**	1.4
	Ribavirin	0.0655 ± 0.001*	28.1	0.0635 ± 0.003*	30.5	0.066 ± 0.001*	27.7
	DMSO	0.091 ± 0.00		0.091 ± 0.000		0.091 ± 0.000	
Mid concentration	Iodixanol	0.056 ± 0.001***	38.8	0.0555 ± 0.001***	39.3	0.058 ± 0.001***	36.6
	Sirolismus	0.0525 ± 0.001*	42.4	0.0545 ± 0.002***	40.5	0.057 ± 0.000***	37.7
	Ribavirin	0.0495 ± 0.002*	46.0	0.046 ± 0.001***	49.4	0.0475 ± 0.001*	48.0
	DMSO	0.091 ± 0.000		0.091 ± 0.000		0.091 ± 0.000	
Highest concentration	Iodixanol	0.0555 ± 0.002*	39.8	0.0535 ± 0.001*	41.6	0.0535 ± 0.001***	41.4
	Sirolismus	0.0535 ± 0.001*	42.2	0.046 ± 0.007*	49.7	0.0545 ± 0.001***	40.3
	Ribavirin	0.045 ± 0.000*	51.4	0.042 ± 0.003*	54.0	0.036 ± 0.009*	60.4
	DMSO	0.092 ± 0.001		0.091 ± 0.000		0.091 ± 0.000	

Values are expressed as mean $\pm$ SEM, n=2.
Two-way ANOVA followed by Dunnet's multiple comparison tests was used.
Values of the group with superscript * are statistically significant ($p<0.05$) compared to negative control group.
Values of the group with superscript ** are statistically significant ($p<0.05$) compared to positive control group.
Values with superscript *** are statistical significant ($p<0.05$) compared to both negative and positive control groups.
The higher %VI the more the antiviral activity of the drug.
Keys: DMSO = Dimethylsulfoxide (Negative control), Ribavirin (Positive control)
%VI = VC-VTG/VC X 100
%VI = Percentage viral inhibition
VC = viral load of the DMSO treated group
VTG = Viral load of the drug treated group
Determination of Selectivity Index of the Two (2) Selected Drugs against Lassa Infected Cell Lines

Table 5: *Selectivity Index of Iodixanol and Sirolismus of Lassa Infected Caco-2 Cells*

	CC_{50} (µg/ml)	IC_{50}(µg/ml)	SI
Lassa	17273	5405	3.20
	1.228	0.4912	2.50
	65.62	11.02	6.0

Keys:
Caco-2 cells- Human epithelia colorectal adenocarcinoma cells
CC_{50} is the concentration that produces 50% cell line viability
IC_{50} is the concentration that produces 50% viral inhibition
$SI = CC_{50}/IC_{50}$ SI= Selectivity Index
Both IC_{50} and CC_{50} were extrapolated using nonlinear regression analysis generated by graph-pad prism.
The higher the SI the more effective and safe a drug would be during treatment

4.0   Discussion

In this study, sirolismus demonstrated a concentration-dependent viral killing effect against Lassa statistically different from the vehicle-treated group in the three different post-treatment time points. Additionally, the maximum virucidal effects was seen in the 48 hours post treatment group indicating that 48 hours is the optimal effective period for sirolismus against Lassa virus. At C_{max} (0.1 µg/ml), the virucidal effects of sirolismus was 11.4%, statistically different from the DMSO treated group. However, the highest virucidal effect (49.7%) at 0.4µg/ml was not statistically different from 54% for ribavirin. Conversely, the IC_{50} of sirolismus against Lassa was 0.5µg/ml, five times greater than the C_{max} (0.1 µg/ml), indicating that sirolismus is less potent for Lassa. Again, the selectivity index for sirolismus against Lassa infected Caco-2 cells was 2.5, signifying a relatively narrow margin of safety against Lassa infected cell line. However, the selectivity index of ribavirin on the other hand was 6.0, implying that ribavirin is more selective for Lassa when compared to sirolismus.

Comparably, sirolismus shared similar pharmacophore features (2 HBA, 2 HBD and 2 hydrophobic interactions) with all the structure and ligand based-pharmacophores generated from the Lassa viral targets. This might be a possible molecular reason for its activity against Lassa. Again, sirolismus had the highest predicted binding affinity (20.4) against Lassa nucleoprotein, hence its mechanism of action against Lassa might be related to high affinity for Lassa nucleoprotein. Additionally, the 3D structure of sirolismus superimposes with the 3D of the respective co-crystalized ligands for three Lassa viral targets, again this might further explain its *In-vitro* anti-Lassa activity.

From the literature search using different search parameters, this study was the first to identify the anti-Lassa effect of sirolismus and iodixanol. However, previous study revealed that solid-organ transplant recipients treated with mTOR inhibitors; sirolimus or everolimus, have fewer clinical Cytomegalovirus (an envelope virus like Lassa) infections than those on other forms of immunosuppression (Nashan, 2018).

Iodixanol on the other hand, demonstrated a concentration-dependent viral killing effect against Lassa statistically different from the vehicle treated group in the three different post-treatment time points. Additionally, the maximal virucidal effect was seen in the 48 hours post treatment group indicating that 48 hours is the optimal effective period for iodixanol against Lassa virus. At C_{max} (1000 µg/ml), the virucidal effect of iodixanol was 5.8%, statistically different from the DMSO treated group. However, the highest virucidal effect (41.6%) at 0.4µg/ml was not statistically different from 54% for ribavirin. Conversely, the IC_{50} of iodixanol against Lassa was 5405 µg/ml, five times greater than the Cmax (1000 µg/ml), indicating that sirolismus is less potent against Lassa. The selectivity index for iodixanol against Lassa infected Caco-2 cells was 3.2, signifying a relatively narrow margin of safety against Lassa infected cell line. However, the selectivity index of ribavirin on the other hand was 6.0, implying that ribavirin is more selective for Lassa as compared to iodixanol.

Comparably, iodixanol shared similar pharmacophore features (2 HBA, 2 HBD and 2 hydrophobic interactions) with all the structure and ligand based-pharmacophores generated from the Lassa viral targets, this might be a possible molecular reason for its activity against Lassa. Again, iodixanol had the highest predicted binding affinity (21.9) against Lassa nucleoprotein, hence its mechanism of action against Lassa might be related to high affinity for Lassa nucleoprotein. Additionally, the 3D structure of iodixanol superimposes with the 3D of the

respective co-crystalized ligands for three Lassa viral targets, again this might further explain its *In-vitro* anti-Lassa activity.

Iodixanol is a non-ionic hydrophilic compound commonly used as a contrast agent during coronary angiography, particularly in individuals with renal dysfunction, as it is believed to be less toxic to the kidneys than most other intravascular contrast agents (Lubbers et al., 2017).

From the literature search using different search parameters, no known study have reported anti-Lassa effect of iodixanol. However, copper iodide, an iodine-containing compound exert Antiviral activity against H1NI influenza by generating hydroxyl radicals (Vincent et al., 2016). Similarly, Povidone iodine solution showed good efficacy against both enveloped and non- enveloped viruses including adenovirus and polyomaviruses (Eggers et al., 2015). Conflictingly, an antimicrobial study revealed iodixanol not to impede bacteria growth in a culture media (Klimentová and Stulík, 2015).

5.0 Conclusion

The result of the study showed that iodixanol and sirolismus produced a concentration dependent viral killing against virus. The low potency and selectivity index of the two drugs against the infected cell line is the issue of concern.

5.1 Recommendations

Further evaluation of the iodixanol and sirolismus against the three viruses using different cell lines followed by in vivo studies at biosafety level IV is recommended. Combination analysis of iodixanol and sirolismus with known anti-retroviral drugs might yield fruitful result.

5.2 Limitations of the study

Because of time limit and financial constraints, this study focus mainly on the measurement of virucidal effect using real time PCR. Combining different methods gives a more robust and validated findings. Other methods include;
(1)   Flow cytometry measurement of specific viral proteins/antigens in the infected supernatant (like Lassa polymerase) by flow cytometry.
(2)   Measurement of viral induced cytopathic effects via cell counting and microscopy

Acknowledgement

References

Akpede, G. O., Asogun, D. A., Okogbenin, S. A. & Okokhere, P. O. 2018. Lassa fever outbreaks in Nigeria. Taylor & Francis.

Ansari, S., Kamali, A. N., Bagherzadeh, K., Amanlou, M. & Aghabalazadeh, S. 2018. Selection of Efficient Inhibitors for Caspas-9 according to Structure-Based Pharmacophore Screening Strategy and Molecular Dynamics Simulations. *Trends in Peptide and Protein Sciences,* 2**,** 35-43.

Bhandari, U. 2017. A Textbook of Pharmacology. *International Journal of Pharmaceutical and Phytopharmacological Research,* 1**,** 140.

Dallakyan, S. & Olson, A. J. 2015. Small-molecule library screening by docking with PyRx. *Chemical Biology.* Springer.

Eggers, M., Eickmann, M., Kowalski, K., Zorn, J. & Reimer, K. 2015. Povidone-iodine hand wash and hand rub products demonstrated excellent in vitro virucidal efficacy against Ebola virus and modified vaccinia virus Ankara, the new European test virus for enveloped viruses. *BMC infectious diseases,* 15**,** 375.

Ellingson, S. R. & Baudry, J. 2014. High-throughput virtual molecular docking with AutoDockCloud. *Concurrency and Computation: Practice and Experience,* 26**,** 907-916.

Farag, M. M. & Mansour, M. T. 2016. Characterization of Subviral Particles of Hepatitis B Virus Produced by HepG2. 2.15 Cell Line-In vitro Study. *International Journal of Virology and Molecular Biology,* 5**,** 1-7.

Kati, W., Koev, G., Irvin, M., Beyer, J., Liu, Y., Krishnan, P., Reisch, T., Mondal, R., Wagner, R. & Molla, A. 2015. In vitro activity and resistance profile of dasabuvir, a nonnucleoside hepatitis C virus polymerase inhibitor. *Antimicrobial agents and chemotherapy,* 59**,** 1505-1511.

Klimentová, J. & Stulík, J. 2015. Methods of isolation and purification of outer membrane vesicles from gram-negative bacteria. *Microbiological research,* 170**,** 1-9.

Kühnert, D., Kouyos, R., Shirreff, G., Pečerska, J., Scherrer, A. U., Böni, J., Yerly, S., Klimkait, T., Aubert, V. & Günthard, H. F. 2018. Quantifying the fitness cost of HIV-1 drug resistance mutations through phylodynamics. *PLoS pathogens,* 14**,** e1006895.

Lo, M. K., Shi, P.-Y., Chen, Y.-L., Flint, M. & Spiropoulou, C. F. 2016. In vitro antiviral activity of adenosine analog NITD008 against tick-borne flaviviruses. *Antiviral research,* 130**,** 46-49.

Lubbers, M. M., Kock, M., Niezen, A., Galema, T., Kofflard, M., Bruning, T., Kooij, H. S., Van Valen, H., Dijkshoorn, M. & Booij, R. 2017. Iodixanol versus Iopromide at Coronary CT Angiography: Lumen Opacification and Effect on Heart Rhythm—the Randomized IsoCOR Trial. *Radiology,* 286**,** 71-80.

Nashan, B. 2018. mTOR inhibition and clinical transplantation: liver. *Transplantation,* 102**,** S19-S26.

Sliwoski, G., Kothiwale, S., Meiler, J. & Lowe, E. W. 2014. Computational methods in drug discovery. *Pharmacological reviews,* 66**,** 334-395.

Smart, O. S., Horský, V., Gore, S., Svobodová Vařeková, R., Bendová, V., Kleywegt, G. J. & Velankar, S. 2018. Worldwide Protein Data Bank validation information: usage and trends. *Acta Crystallographica Section D,* 74**,** 237-244.

Tambo, E., Adetunde, O. T. & Olalubi, O. A. 2018. Re-emerging Lassa fever outbreaks in Nigeria: Re-enforcing "One Health" community surveillance and emergency response practice. *Infectious diseases of poverty,* 7**,** 37.

Vincent, M., Hartemann, P. & Engels-Deutsch, M. 2016. Antimicrobial applications of copper. *International journal of hygiene and environmental health,* 219**,** 585-591.

Wang, P., Liu, Y., Zhang, G., Wang, S., Guo, J., Cao, J., Jia, X., Zhang, L., Xiao, G. & Wang, W. 2018. Screening and Identification of Lassa Virus Entry Inhibitors from an FDA-Approved Drugs Library. *Journal of virology***,** JVI. 00954-18.

Wishart, D. S., Feunang, Y. D., Guo, A. C., Lo, E. J., Marcu, A., Grant, J. R., Sajed, T., Johnson, D., Li, C. & Sayeeda, Z. 2017. DrugBank 5.0: a major update to the DrugBank database for 2018. *Nucleic acids research,* 46**,** D1074-D1082.

Yamani, L. N., Yano, Y., Utsumi, T., Wasityastuti, W., Rinonce, H. T., Widasari, D. I., Lusida, M. I. & Hayashi, Y. 2017. Profile of Mutations in the Reverse Transcriptase and Overlapping Surface Genes of Hepatitis B Virus (HBV) in Treatment-Naïve Indonesian HBV Carriers. *Japanese journal of infectious diseases,* 70**,** 647-655.